



OPEN

Robotic trunk perturbation magnitude affects standing postural responses in individuals with motor complete spinal cord injury receiving epidural stimulation

Enrico Rejc^{1,2}✉, Collin D. Bowersock³, Tanvi Pisolkar⁴, Simone Zaccaron^{2,5},
Claudia A. Angelis¹, Gail F. Forrest^{1,6}, Sunil Agrawal^{7,8} & Susan J. Harkema¹

After a severe spinal cord injury (SCI), the human spinal circuitry receiving epidural stimulation can generate lower limb postural responses to sensory inputs associated with trunk perturbation. Here, we assessed the effects of different trunk perturbative forces on standing postural responses in six individuals with chronic, motor complete SCI receiving epidural stimulation to facilitate standing. The robotic upright stand trainer (RobUST) provided constant assistance for pelvic control and delivered precise trunk perturbations with different magnitudes ($10 \pm 4\%$ BodyWeight (BW) -Low, $14 \pm 4\%$ BW -Mid, and $18 \pm 4\%$ BW -High) and directions (left, right, front, back). Trunk excursion, ground reaction forces (GRF), and electromyography (EMG) amplitude were assessed. Perturbation magnitude significantly affected trunk excursion and GRFs in all tested directions ($p \leq 0.002$), with larger modulations elicited by higher perturbation magnitudes. Lower limb EMG amplitude responses were less consistent. In some instances, perturbation magnitude did not affect EMG amplitude. In others, high-magnitude perturbations promoted larger EMG amplitude modulation compared to weaker perturbations, resulting in higher or lower levels of activation depending on muscle and direction. These findings contribute to characterize the residual postural control potential of the human spinal circuitry below the level of SCI, which should be considered when defining postural training protocols with spinal cord neuromodulation.

Keywords Epidural stimulation, Spinal cord injury, Postural control, Robotics, Perturbations, Standing

A growing body of literature supports the view that spinal cord epidural stimulation (scES) combined with activity-based training can promote significant recovery of lower limb motor function for standing and walking in individuals that were paralyzed because of a chronic, clinically motor complete spinal cord injury (SCI)¹⁻⁵. scES modulates the excitability of spinal circuitry by activating primarily large somatosensory fibers⁶⁻⁹, so that sensory information and residual supraspinal inputs (that are not functional when stimulation is turned off) can serve as sources of motor control^{3,10-12}. Upright postural control is critical for the successful execution of many different motor tasks including standing and walking¹³. Spinal cord injury also disrupts postural control¹⁴, and it

¹Tim and Caroline Reynolds Center for Spinal Stimulation, Kessler Foundation, 1199 Pleasant Valley Way, West Orange, NJ 07052, USA. ²Department of Medicine, University of Udine, Udine, Italy. ³Human Performance and Nutrition Research Institute, Oklahoma State University, Stillwater, OK, USA. ⁴Kentucky Spinal Cord Injury Research Center, University of Louisville, Louisville, KY, USA. ⁵Department of Neurosciences, Biomedicine and Movement Sciences, University of Verona, Verona 37129, Italy. ⁶Department of Physical Medicine and Rehabilitation, Rutgers New Jersey Medical School, Newark, NJ, USA. ⁷Department of Mechanical Engineering, Columbia University, New York, NY, USA. ⁸Department of Rehabilitation and Regenerative Medicine, Columbia University, New York, NY, USA. ✉email: erejc@kesslerfoundation.org; enrico.rejc@uniud.it

is still unclear whether, and to what extent, the human spinal circuitry below the level of injury, receiving scES, can interpret sensory information and generate effective lower limb postural responses.

Animal model studies propose that posture is controlled by the interaction between supraspinal and spinal control systems^{15–17}, the latter being more involved in receiving inputs from the limb sensory receptors and generating corrective motor responses¹⁸. When supraspinal inputs are disrupted by SCI, spinal postural control relies on the integration of limb-related somatosensory information to adjust posture¹⁹. Further evidence from animal models that are spinalized and/or decerebrated suggests that spinal cord neuromodulation and postural training may promote partial recovery of postural control^{19–22}.

Consistent with the observation from animal models, individuals with motor complete SCI receiving scES to facilitate standing (Stand-scES) can modulate lower limb muscle activation pattern by body weight shifting during standing^{2,23}. To further assess the residual postural control potential in this population, we leveraged on a dedicated cable-driven robotic upright stand trainer (RobUST)²⁴. We observed that the human spinal circuitry can respond to trunk perturbations with lower limb activation amplitude and patterns that were, respectively, higher and generally more appropriate when the research subjects did not hold the fixed handlebars for self-balance assistance (i.e., free hands)²⁵. These findings suggest that the human spinal circuitry interpreted sensory information related to trunk displacement and ground reaction force, which were also modulated to a greater extent with free hands.

With this in mind, we implemented RobUST to train standing postural control with free hands in six individuals with high-level motor complete SCI who had previously practiced stand training with Stand-scES using a walker or standing frame. Robotic stand training with Stand-scES, consisting of steady and dynamic tasks performed with assistance-as-needed and trunk perturbations, substantially improved steady and dynamic standing postural control while the participants received only external assistance for pelvic control²³. Conversely, robotic stand training did not affect the control of similar steady and dynamic postural control tasks tested in sitting, suggesting that posture-specificity may contribute to the characteristics of motor re-learning²⁶.

Overall, these findings highlight the importance of further understanding whether and how the human spinal circuitry can interpret peripheral sensory information related to different postural perturbation characteristics to modulate the resulting activation patterns enabled by scES. Here, we have approached this topic by investigating the effects of sensory inputs associated with different (i.e., graded) trunk perturbative forces delivered by RobUST on standing postural responses facilitated by Stand-scES. Our hypothesis was that larger trunk perturbation magnitude would promote larger trunk excursion and ground reaction forces, which would result in larger EMG amplitude modulation.

Materials and methods

Participants

Six individuals with chronic, high-level motor complete SCI who were already implanted with a scES unit for the recovery of motor function consisting of an electrode array with 16 contacts (Medtronic Specify 5–6 – 5 lead) and a neurostimulator (Medtronics, Intellis in participants A96, A101, A82, B45 and B07; RestoreADVANCED in participant B23)², participated in this study (Table 1). These individuals had previously practiced standing with Stand-scES using a standing apparatus or walker²⁷ (140 ± 68 training sessions; 5 sessions / week; 1–2 h per session) as well as robotic postural stand training with RobUST²³ (80 ± 10 training sessions; 5 sessions / week; 1 h per session) as part of other interventional studies, demonstrating their ability to achieve bilateral independent knees extension. This study was conducted according to the standards set by the Declaration of Helsinki and was approved by the University of Louisville Institutional Review Board (IRB #17.1024). Written informed consent was obtained from all study participants.

Spinal cord epidural stimulation parameters to facilitate standing

Tonic scES was implemented in this study to facilitate standing. Individual- and task-specific stimulation parameters (Stand-scES, Supplemental Fig. 1) were selected based on the guidelines reported in previous publications by our group^{1,28,29}. All participants had undergone the process of selection of Stand-scES parameters prior to the beginning of the present study because of the enrollment in previous interventional protocols that included standing. Briefly, the individualized map of motor pools activation deriving from spatiotemporal mapping of spinal cord motor-evoked responses^{29–31} was considered to determine the initial electrode configuration, adjusting the position of cathodes in order to target primarily extensors muscle groups while

Pub ID	Age (Yrs)	Sex	Time since injury (Yrs)	Level of Injury	AIS	Time since scES implant (Yrs)
A96	29	F	5.3	C4	A	1.7
A101	33	M	4.2	C3	A	1.6
A82	37	M	8.8	C4	A	1.2
B45	36	M	9.3	C7	B	0.3
B07	35	M	14.4	T2	B	11.0
B23	38	M	9.4	C4	B	6.1

Table 1. Research participants' characteristics. Pub ID: publication identifier; F: female; M: male; Level of injury: neurological level of the lesion by AIS (American Spinal Injury Association (ASIA) Impairment Scale); C: cervical; T: thoracic; scES: spinal cord epidural stimulation.

limiting the activation of primary flexor muscles. Additionally, the topographical organization of the activation pattern³⁰ and previous evidence that cathodes positioned in the caudal area of the lumbosacral spinal cord, and more caudal than the anodes, can promote better motor pattern for standing^{32,33} were also considered. Further, near-motor threshold stimulation intensities, which did not elicit directly lower limb movements in sitting, were selected and delivered at the highest stimulation frequencies that promoted effective extensor activation patterns to bear body weight.

Robotic upright stand trainer

RobUST, and its implementation in individuals with SCI that are unable to stand independently, were described in detail in previous publications^{24,25,34}. Briefly, 12 DC motors (Maxon Motor, Switzerland) mounted on the RobUST metal frame applied forces to a customized harness worn by the research participant *via* cables that are routed through a pulley system. Planar forces, measured by dedicated load cells (LSB302 Futek, CA), were applied by four cables attached to the trunk harness and by other four cables to the pelvis harness. Two force platforms (Bertec, Columbus, OH) embedded in a wooden frame were implemented to collect ground reaction forces. Eight infrared cameras mounted on the RobUST metal frame (Vicon Bonita 10; Denver, CO) were connected to the motion capture system to track the instantaneous position of reflective markers placed at the back of the trunk and pelvis harnesses and on the shoulder straps for kinematic analysis and proper functioning of the robotic device.

Experimental procedures

Stand-scES was turned on while the research participant was seated onto their wheelchair, immediately prior to the sit to stand transition, and remained on during the entire experimental session. RobUST was configured to provide constant assistance for pelvic control and deliver precise trunk perturbation forces while participants receiving Stand-scES were standing with independent lower limbs extension (A96, A101, A82, B45, B23), or with manual assistance by a trainer to promote knee extension (B07), without placing their hands on the handlebars for balance assistance (i.e., free-hands) (Fig. 1A). As reported in previous publications by our group^{23,25,26}, a constant force of 80 N was applied to the pelvis harness to facilitate appropriate hip extension and pelvic tilt, with additional manual assistance implemented by trainers as needed. This constant force level was found optimal to stabilize pelvis while allowing it to safely move when excessive forces were generated (i.e., unexpected muscle spasms). Also, RobUST trunk motors exerted a low-level constant force (30 N) to optimize the delivery

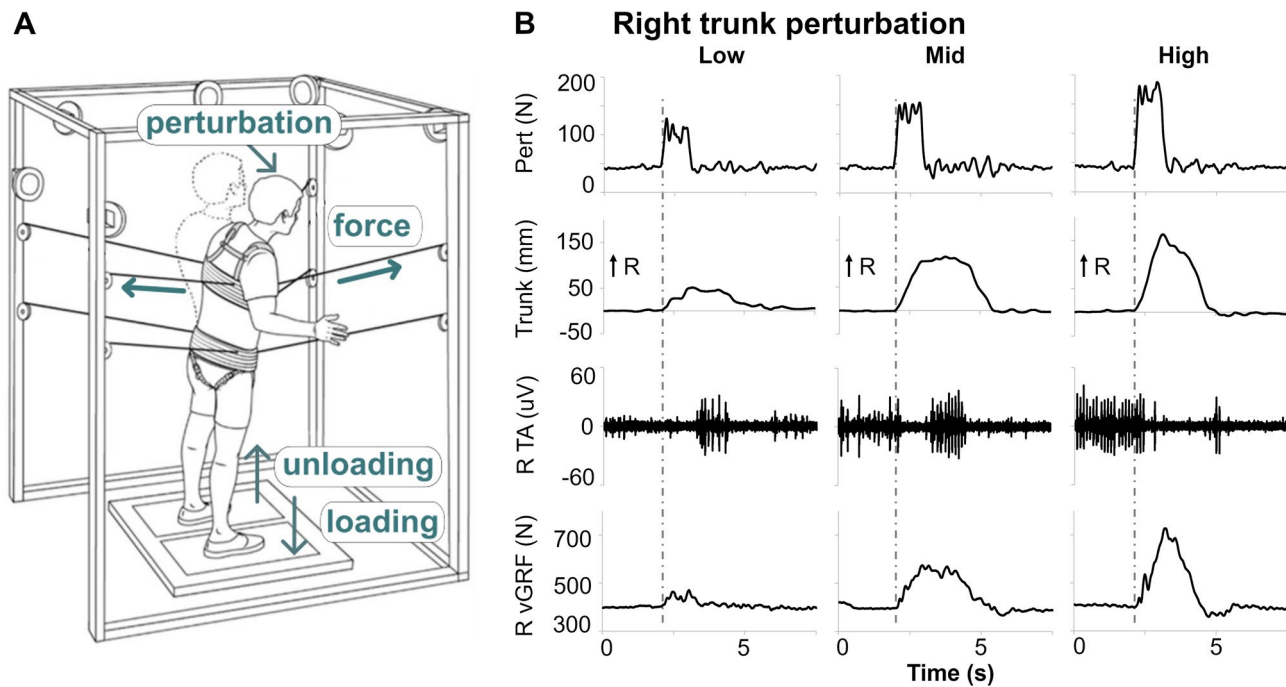


Fig. 1. (A) Schematic of the Robotic Upright Stand Trainer (RobUST) delivering a right trunk perturbation. Perturbative forces are generated by mounted motors and delivered by cables attached to the trunk harness. Pelvis motors and cables apply constant force to assist pelvic control. Trunk kinematic and ground reaction forces are collected through motion capture cameras mounted on the frame and two force platforms, respectively (modified from Rejc et al.²⁶). (B) Representative kinematic, electromyography (EMG) and kinetic responses from participant B45 to right trunk perturbations delivered at Low (7%Bodyweight, BW), Mid (11%BW) and High (15%BW) magnitude. Trunk displacement (Trunk) toward the right (R) side and R leg vertical ground reaction force (vGRF) change from baseline are larger with larger perturbation magnitudes (Pert). Vertical grey dotted lines depict perturbation onset. TA: tibialis anterior.

of perturbative forces without eliciting trunk movement. The perturbation forces applied to the trunk were characterized by a trapezoidal time course with 0.15 s rise time, 0.8 s constant time, and 0.15 s fall time.

The magnitudes of trunk perturbation forces, defined as percentage of participant's body weight (BW, N), were selected during an acclimation session based on information that was previously collected. In summary, the perturbation forces defined as safe and challenging for each participant in a previous study²⁵ were initially implemented, and gradually increased to identify the highest forces that could be safely applied across perturbation directions (left, right, front, back). Such value defined the High perturbation magnitude ($18 \pm 4\%$ BW). Mid ($14 \pm 4\%$ BW) and Low ($10 \pm 4\%$ BW) perturbation were then defined by subtracting 4%BW and 8%BW, respectively, to the High magnitude value of each individual. Low, Mid and High trunk perturbation forces were tested four times for each direction (left, right, front, back) in a randomized order; perturbation direction was not disclosed. Perturbation onset was always preceded by a 3-second countdown. Perturbations were deemed successful if the research participant regained and/or maintained the standing posture for at least 3 s after the end of a perturbative force application, without the need of any additional external assistance including the use of handlebars for balance assistance. Only successful perturbations were considered for further analysis.

Data acquisition

As reported in previous publications^{23,25}, motor force, kinematic data, force platforms data, and electromyography (EMG) of trunk and lower limb muscles were collected in this study. Load cells were connected to a LabVIEW PXI system (National Instruments, Austin, TX) to record the force generated by each motor at 200 Hz. Vicon Nexus motion capture system (Vicon, Denver, CO) recorded trunk kinematics at a sample rate of 100 Hz. Ground reaction forces measured by two independent force platforms were collected in the Vicon Nexus system at 1000 Hz. EMG activity of right (R) and left (L) upper trapezius (UT), adductor (AD), vastus lateralis (VL), medial hamstring (MH), tibialis anterior (TA), medial gastrocnemius (MG) was recorded by bipolar surface electrodes with a fixed inter-electrode distance (17 mm) at 2000 Hz using a dedicated acquisition system (Motion Lab Systems, Baton Rouge, LA) and custom-written software (National Instruments, Austin, TX).

Data analysis

As previously reported²⁵, during offline data analysis, a low-pass filter was applied to motor and force plate data with a cutoff frequency of 25 Hz^{25,35}. Kinematic data of the trunk geometrical center, which was used to estimate trunk excursion²⁴, was low-pass filtered at 6 Hz. EMG data was band-pass filter (20–500 Hz), rectified, and then lowpass filtered (25 Hz)²⁵. As previously reported²⁵, left and right perturbations were grouped into lateral perturbations with kinematic, kinetic, and EMG variables expressed as ipsilateral or contralateral to the perturbation direction. Front and back perturbations were analyzed independently. Outcomes considered for analysis were trunk excursion, percent change from baseline in peak vertical ground reaction forces (vGRF) and peak resultant horizontal ground reaction forces (hGRF), percent change from baseline in EMG amplitude, and the rate of EMG response types (i.e., increased activation, no change, or inhibition compared to baseline).

Baseline data were assessed over a 1.5-second time window from 2.2 to 0.7 s prior to perturbation onset, while perturbation responses were assessed within a 3-second time window starting at perturbation onset²⁵. Perturbation onset coincided with the time point at which the perturbation force was larger than the average baseline force plus three standard deviations. Trunk excursion was defined as the maximum resultant displacement of the trunk's geometrical center in response to the perturbation²⁴. For each time point, the resultant displacement of the trunk's geometrical center was calculated as:

$$\text{Trunk excursion}(t) = \sqrt{(AP_d(t))^2 + (ML_d(t))^2} \quad (1)$$

where AP_d is the trunk displacement in the anteroposterior direction, and ML_d is the trunk displacement in the mediolateral direction. The maximum value of this resultant displacement over the time window considered for analysis was then used to define trunk excursion. The percent change in vGRF and hGRF from baseline was calculated as follows. For lateral perturbations, ipsilateral and contralateral vGRF and hGRF were calculated by the left and right force plates data, to define the amount of loading and unloading as well as hGRF modulation induced by trunk perturbation. For front and back perturbations, the total force recorded from the two force plates was used to determine vGRF and hGRF modulation.

The EMG amplitude percent change from baseline was assessed by using a 1.5-second sliding window over the 3-second time window starting at the perturbation onset, with a 0.025-second overlapping window. For each muscle and perturbation, the 1.5-second window with the maximum integrated EMG detected over the 3-second window was considered for analysis. Also, this maximum integrated EMG was used to classify the EMG response type. EMG responses that were larger than the baseline EMG integral plus three standard deviations were considered as “increased activation”. Responses that were less than the baseline EMG integral minus three standard deviations were considered as “inhibition”. All other responses were considered as “no change” from baseline.

Statistical analysis

Statistical analysis was performed using JASP (Version 0.18, Netherlands). Results are reported as mean and standard error. Participants that demonstrated at least one successful perturbation for all tested conditions (Low, Mid and High perturbation magnitude) within each perturbation direction (lateral, front or back) contributed to the related results and statistical comparisons. The effects of trunk perturbation magnitude on trunk excursion, ground reaction forces and EMG amplitude were analyzed within lateral, front and back perturbations with linear mixed models that included a random intercept for individual variability, and subsequent Bonferroni post

hoc test. The model assumptions of normality, linearity, homoskedasticity, and independence were checked. If these assumptions were violated, log-transformation was applied to trunk excursion and ground reaction force data, or outliers (i.e., data points that were > 2.5 standard deviations far from the mean distribution) were removed for EMG amplitude variables, as they presented both negative and positive values and could not be reliably transformed. If this approach was not sufficient, within-subject repeated observations were averaged to result in one data point per participant. In this case, the effect of perturbation magnitude was tested with one-way repeated measures ANOVA. Sphericity was verified by Mauchly's test. When the assumption of sphericity was not met, the significance of the F-ratios was adjusted according to the Greenhouse-Geisser procedure. When significant differences were found, a Bonferroni post hoc test was used to determine the location of the difference. In case of violation of the assumption of normality, Friedman test and subsequent Conover's post hoc tests were implemented. All tests were 2 sided. Within each perturbation direction and muscle, we also used a 3×3 chi-square test of independence to determine the effect of perturbation magnitude (Low, Mid, High) on the rate of EMG response type (increased activation, no change, inhibition). Post hoc analyses were performed using adjusted residuals with absolute values greater than 2 to determine specific significant differences. For all tests, the statistical significance level was set as $p < 0.05$. To quantify the obtained estimates, a linear model equivalence to Cohen's d^{36} effect size (ES) was calculated as the test statistic divided by the square root of the sample size (i.e., $ES = t / \sqrt{n}$). Sawilowsky's extension³⁷ to Cohen's criteria was used to classify the obtained effect sizes as small (0.2–0.49), median (0.5–0.79), large (0.8–1.19), very large (1.2–1.99), and huge (> 2.0). A post-hoc analysis to assess statistical power (Power) was conducted using the calculated effect size and the study sample size.

Results

We found consistent effects of trunk perturbation magnitude on the kinematic and kinetic variables of this study, with larger trunk excursion and larger GRF modulation brought about by larger perturbation magnitudes. Figure 1B exemplifies this trend for participant B45, receiving right trunk perturbations at 7%BW, 11%BW and 15%BW, respectively, and demonstrating a parallel increase in trunk excursion and loading (vGRF) of the limb ipsilateral to the perturbation direction. Group data for lateral perturbations (Fig. 2A) confirmed these relevant differences ($p < 0.001$ between each comparison), including the larger unloading for the leg contralateral to perturbation direction, which ranged between 10% (ipsilateral vGRF, Mid vs. High: $ES = 2.06$, Power = 98%) and 163% (trunk excursion, Low vs. High: $ES = 5.40$, Power = 100%), with higher perturbation magnitudes.

EMG amplitude modulation was generally less consistent. No significant effect of perturbation magnitude was found on contralateral EMG amplitude (Fig. 2C). However, High-magnitude perturbations resulted in reduced ipsilateral VL EMG amplitude response compared to the weaker magnitudes (~ -17%, $ES = 0.99$, $p = 0.045$, Power = 50%; Fig. 2A). A similar trend, exemplified in Fig. 1B for participant B45, was also found for ipsilateral TA (Fig. 2A). Conversely, the ipsilateral UT (upper trunk muscle that could be voluntarily activated) showed higher EMG amplitude (25%, $ES = 1.18$, $p = 0.011$, Power = 64%) with High perturbation compared to Low (Fig. 2B).

The analysis of rate of EMG response type (i.e., increased activation, no change, or inhibition compared to baseline) showed an effect of perturbation magnitude for contralateral VL ($p = 0.047$) and MG ($p = 0.004$; Fig. 3). For both muscles, Low perturbation magnitude resulted in significantly more responses without EMG modulation (no change) as well as less frequent inhibition responses, compared to the Mid and High magnitudes. Contralateral MG also showed a lower rate of no change responses with High perturbations compared to weaker magnitudes.

Larger trunk excursion and hGRF were also promoted by larger perturbation magnitudes during back perturbations (Figs. 4 and 5A). The related significant differences ranged from 27% in hGRF (Mid vs. High: $ES = 1.16$, $p = 0.028$, Power = 50%) to 132% in trunk excursion (Low vs. High: $ES = 2.66$, $p < 0.001$, Power = 99%). Furthermore, as exemplified in Fig. 4 for participant A96, the antagonist ankle muscles, TA and MG, showed opposite trends of EMG amplitude modulation at increasing magnitudes. Specifically, MG EMG amplitude significantly decreased during higher perturbation magnitudes (Low vs. High: $ES = 2.03$, $p < 0.001$, Power = 92%; Mid vs. High: $ES = 1.33$, $p = 0.009$, Power = 61%), indicating inhibition relative to baseline. Conversely, TA EMG amplitude was significantly higher with High ($ES = 1.49$, $p = 0.032$, Power = 71%) compared to Low trunk perturbations (Fig. 5B). No effect of back perturbation magnitude on the rate of EMG response type was noted (Fig. 5C).

An effect of perturbation magnitude during front perturbations was observed for kinematic and kinetic variables, with greater perturbation magnitudes leading to larger trunk excursion and higher hGRF (Fig. 6A). The related differences of these changes ranged from a 12% increase in hGRF, (Low vs. Mid: $ES = 1.94$, $p = 0.002$, Power = 45%) to a 124% increase in trunk excursion (Low vs. High: $ES = 2.23$, $p < 0.001$, Power = 54%). Also, statistical trends of higher EMG amplitude promoted by High perturbations were found for AD ($p = 0.078$; Low vs. High $ES = 1.28$, Power = 25%) and VL ($p = 0.085$; Low vs. High $ES = 1.24$, Power = 24%) (Fig. 6B). No meaningful trends were observed for EMG response types across perturbation magnitudes (Fig. 6C).

Discussion

This study showed that the precise trunk perturbation magnitudes delivered by RobUST resulted in distinct modulation of trunk kinematic and GRF of individuals with high-level motor complete SCI receiving Stand-SCS, with larger trunk excursion and larger GRF brought about by larger perturbation magnitudes. EMG amplitude modulation was less consistent, with some significant effects of perturbation magnitude that were muscle- and direction-specific.

In the mammalian nervous system impacted by SCI, peripheral sensory information received by the spinal circuitry plays a critical role in shaping the muscle activation pattern generated as well as the characteristics

Lateral perturbations

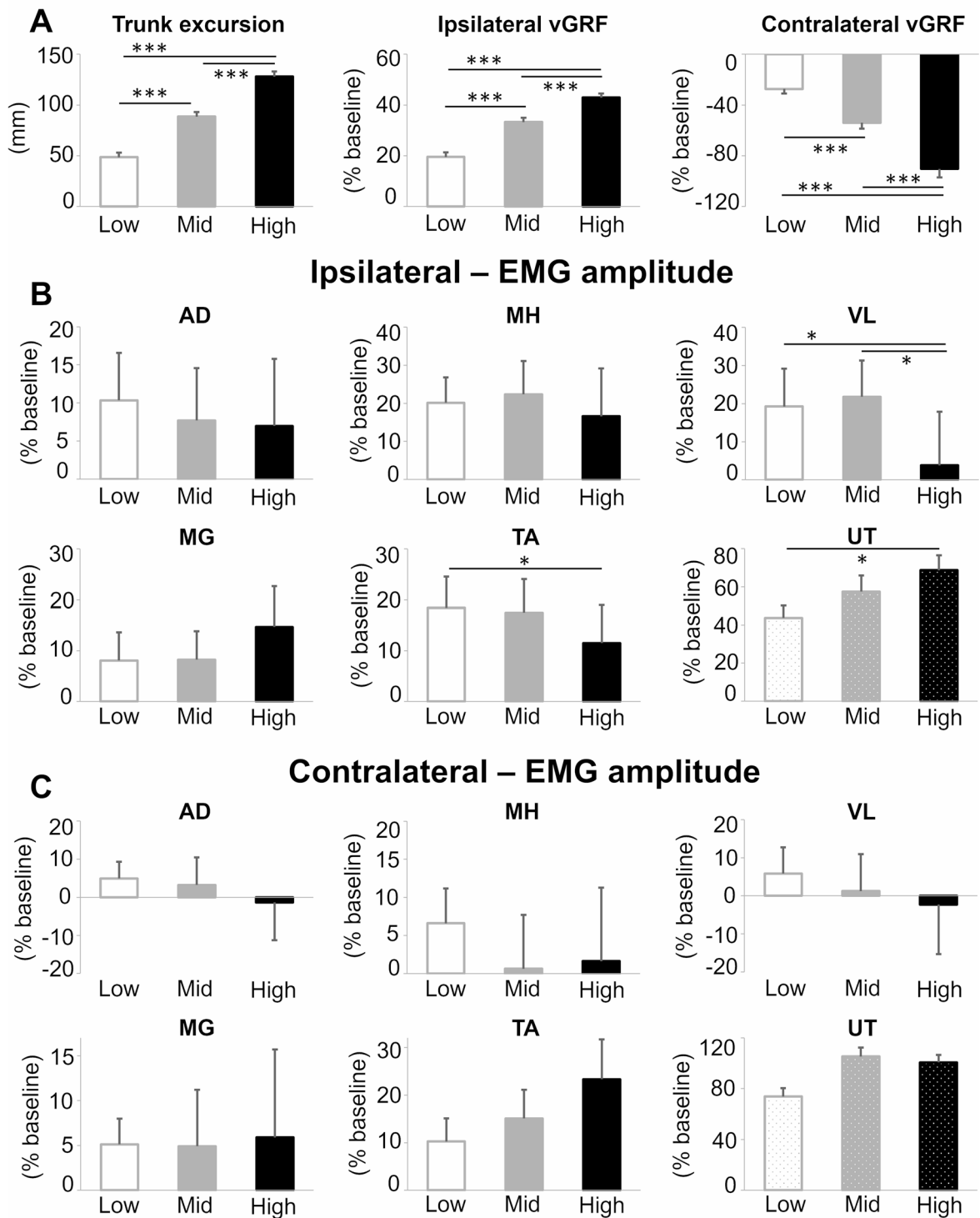


Fig. 2. Group averages during lateral perturbations at Low, Mid and High magnitude for (A) trunk excursion and vertical ground reaction force (vGRF), and electromyography (EMG) amplitude of the (B) ipsilateral and (C) contralateral side to the perturbation direction. AD: adductor magnus; MH: medial hamstring; VL: vastus lateralis; MG: medial gastrocnemius; TA: anterior tibialis; UT: upper trapezius. Error bars represent the standard error. Successful attempts considered for analysis were 43 for Low, 44 for Mid, and 31 for High perturbations collected from 5 participants. Significant difference: * $p < 0.05$; *** $p < 0.001$.

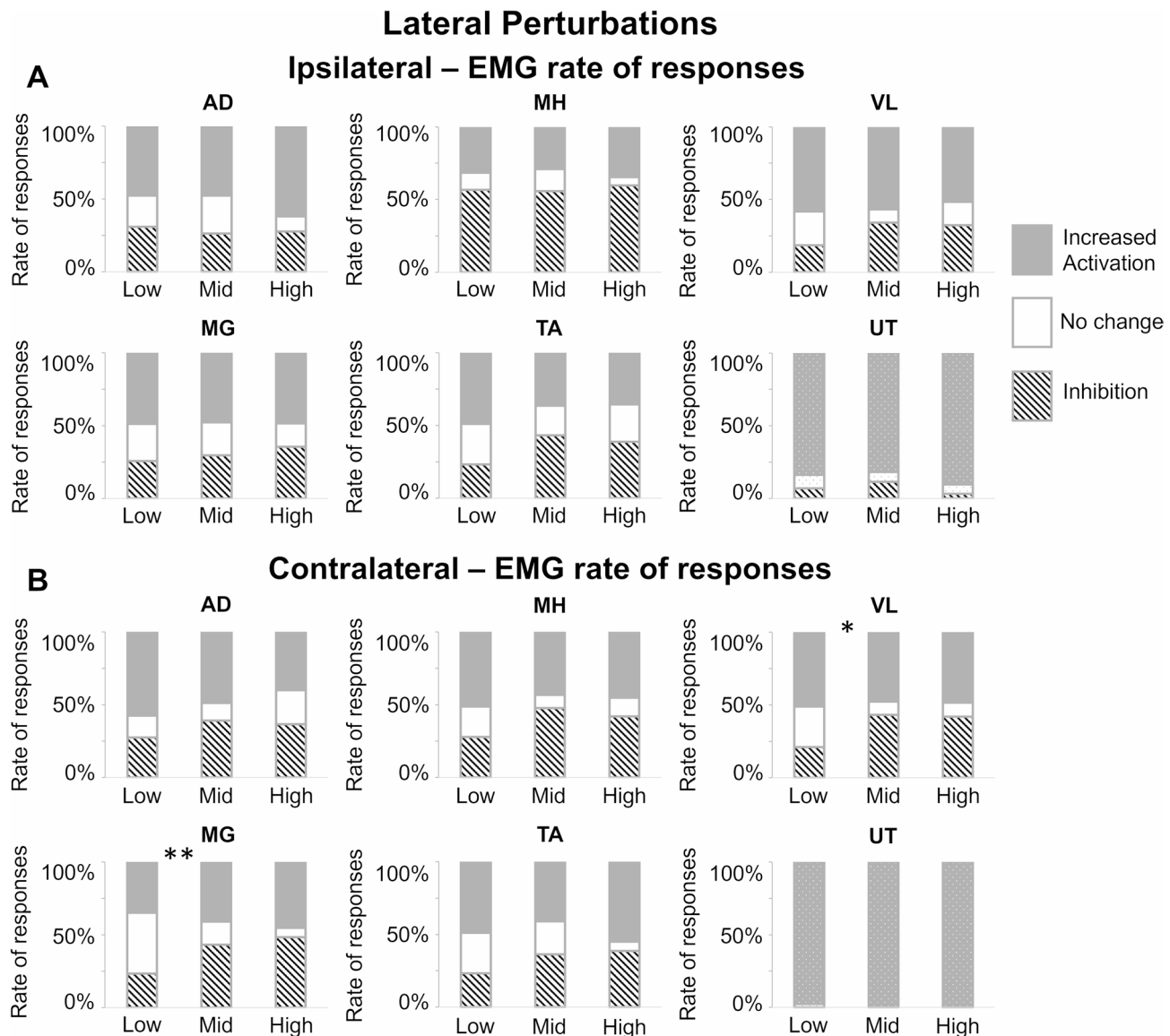


Fig. 3. Rate of electromyography (EMG) response types assessed during lateral trunk perturbations at Low, Mid and High magnitude for muscles (A) ipsilateral and (B) contralateral to the perturbation direction. Grey bars represent increased activation compared to baseline, white indicates no change, and striped indicates inhibition. AD: adductor magnus; MH: medial hamstring; VL: vastus lateralis; MG: medial gastrocnemius; TA: anterior tibialis; UT: upper trapezius. Low magnitude trunk perturbations resulted in significantly more responses with no change as well as less responses showing inhibition for the contralateral VL and MG compared to Mid and High. Contralateral MG also showed less no change responses with High magnitude compared to Mid and Low. Successful attempts considered for analysis were 43 for Low, 44 for Mid, and 31 for High perturbations collected from 5 participants. Significant difference: * $p < 0.05$; ** $p < 0.01$.

of potential motor recovery^{38,39}. scES contributes to this framework by modulating the level of excitability of the spinal circuitry, mimicking the tonic supraspinal drive lost after SCI, so that sensory information could serve as a source of control for generating appropriate motor patterns^{10,11}. However, the injured spinal cord processes sensory information and generates the related motor outputs in an altered manner as a result of injury-related adaptations¹⁰. This can impact the extent to which the human spinal circuits can interpret small changes in perturbation-related sensory information as well as can finely modulate the associated muscle activation responses.

The first step to elucidate this aspect of residual postural control potential was to implement a technology capable of fine-tuning postural perturbation-related sensory information in humans with motor complete SCI receiving scES to facilitate standing. Here, RobUST was able to manipulate perturbation magnitude to control aspects of sensory inputs related to progressively larger trunk displacement as well as larger vertical GRF modulation of the loaded and unloaded leg (i.e., ipsilateral and contralateral side to the perturbation, respectively) during lateral trunk perturbations (Figs. 1 and 2A). Similarly, horizontal GRF generated during

Back trunk perturbation

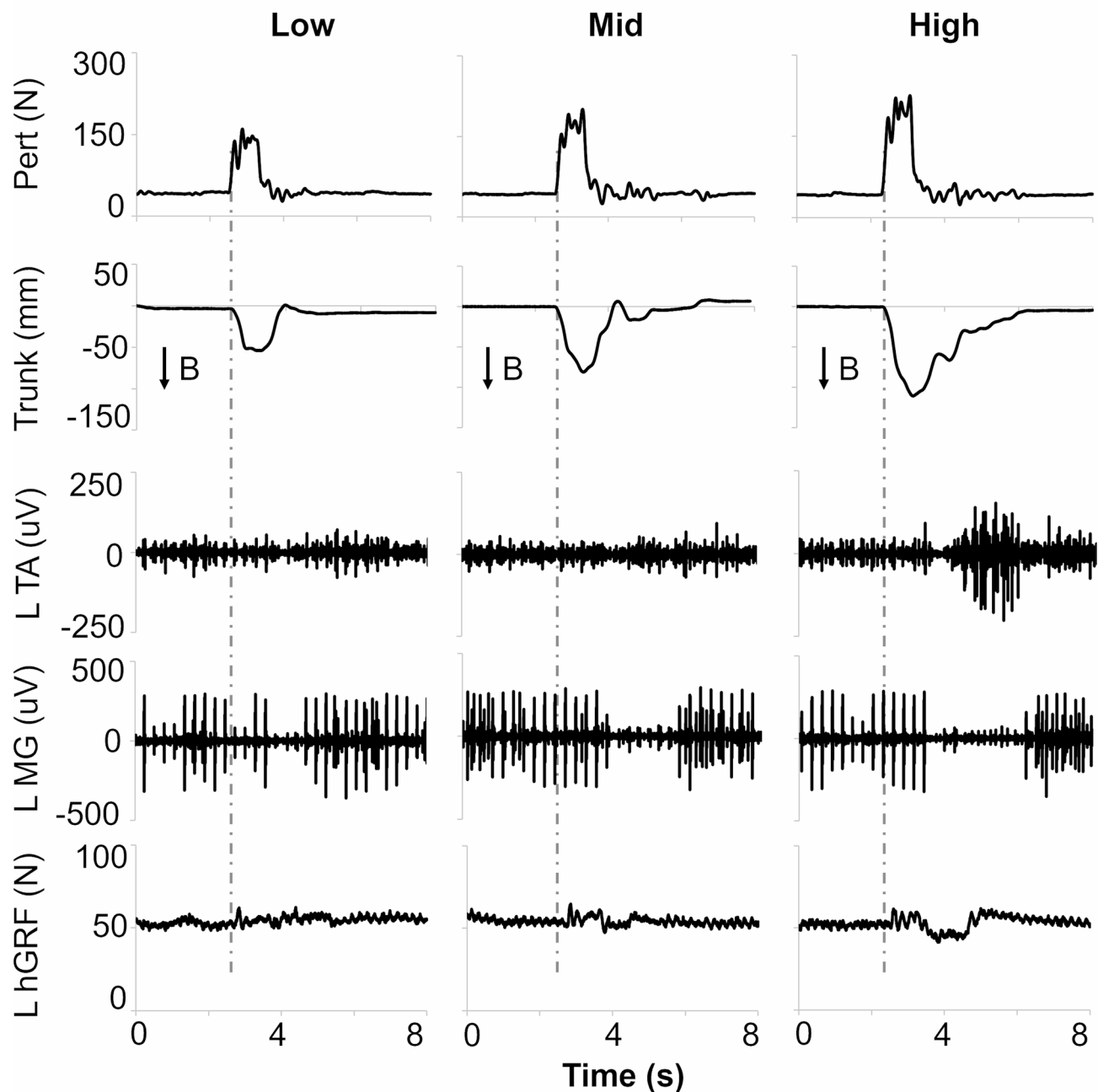


Fig. 4. Representative kinematic, electromyography (EMG) and kinetic responses from participant A96 to back trunk perturbations delivered at Low (12%Bodyweight, BW), Mid (16%BW) and High (20%BW) magnitude. Vertical grey dotted lines depict perturbation onset. Pert: perturbation magnitudes; Trunk: trunk displacement toward the back (B); L: left; TA: tibialis anterior; MG: medial gastrocnemius; hGRF: resultant horizontal ground reaction force. Note the different trends of EMG amplitude modulation for TA (i.e., increased EMG amplitude at High) and MG (i.e., longer inhibition) with increasing perturbation magnitude.

antero-posterior perturbations were directly related to trunk perturbation magnitudes (Figs. 5A and 6A). Such modulation of kinematic and kinetic responses was achieved by small changes in trunk perturbation magnitude (4%BW between Low-Mid and Mid-High conditions) while RobUST also assisted pelvis control by applying constant forces to the dedicated soft pelvic harness. This framework enabled individuals with high-level motor complete SCI and impaired trunk control to have their standing posture safely challenged while their hands were not placed on a fixed handlebar for balance control (i.e., free hands). This is relevant because we recently demonstrated in this population that lower limb postural responses were affected by hands placement, being overall larger and more appropriately modulated when the participants' hands were free²⁵.

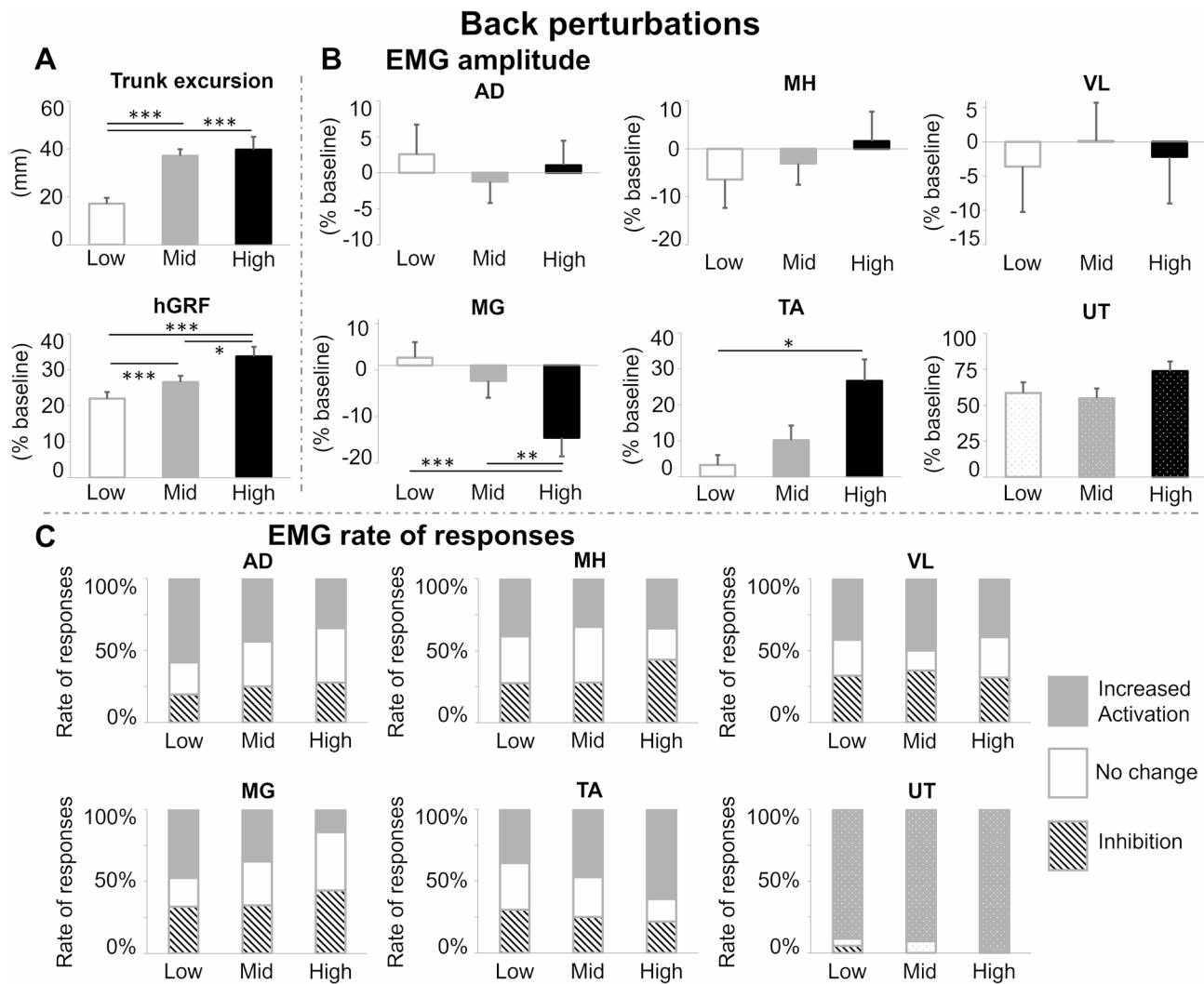


Fig. 5. Group averages during back trunk perturbations at Low, Mid and High magnitude for (A) trunk excursion and horizontal ground reaction force (hGRF), (B) electromyography (EMG) amplitude, and (C) rate of EMG response types. AD: adductor magnus; MH: medial hamstring; VL: vastus lateralis; MG: medial gastrocnemius; TA: anterior tibialis; UT: upper trapezius. Error bars represent the standard error. Successful attempts considered for analysis were 20 for Low, 18 for Mid, and 16 for High perturbations collected from 5 participants. Each attempt contributed to one data point for trunk excursion and two data points (i.e., left and right side) for ground reaction force and EMG amplitude. Significant difference: * $p < 0.05$; ** $p < 0.01$; *** $p < 0.001$.

Using this robotic framework, the relationship between perturbation magnitude and lower limb EMG amplitude (i.e., motor output) was less consistent than the graded response observed for trunk displacement and GRF (i.e., sensory input). An interesting pattern was observed during lateral perturbations, where High magnitude reduced the EMG amplitude of the ipsilateral (i.e., loaded) VL and TA (Figs. 1B and 2B). Generally, it would be expected that these larger postural displacements, evidenced by the increase in trunk excursion and weight shifting, would lead to increased activation of the VL, a knee extensor, and the TA to stabilize the ankle joint. Further, no other lower limb muscle significantly increased its rate of activation during the High magnitude perturbations (Fig. 3). On the other hand, Low-magnitude lateral perturbations promoted a smaller rate of EMG amplitude modulation in the contralateral VL and MG compared to Mid and High (Fig. 3B).

We previously reported that the sensory information related to increased leg loading from sitting to full weight bearing standing contributes to the robust extensor pattern generated by lower limb muscles in individuals with motor complete SCI receiving tonic Stand-scES¹. In a case of motor recovery promoted by years of activity-based training with scES after chronic motor complete paralysis, EMG amplitude of VL and MG was larger during unilateral weight bearing compared to bipedal weight bearing during standing, whereas MH and TA did not show EMG amplitude modulation consistent with the different leg loading between conditions⁴⁰. Also, adjustments of %BW support while stepping on a treadmill modulated EMG amplitude of lower limbs in individuals with SCI⁴¹. Direct relationships between vGRF and EMG amplitude were particularly consistent for the soleus and MG muscles at leg loading levels lower than 50%BW, whereas a much weaker relationship or

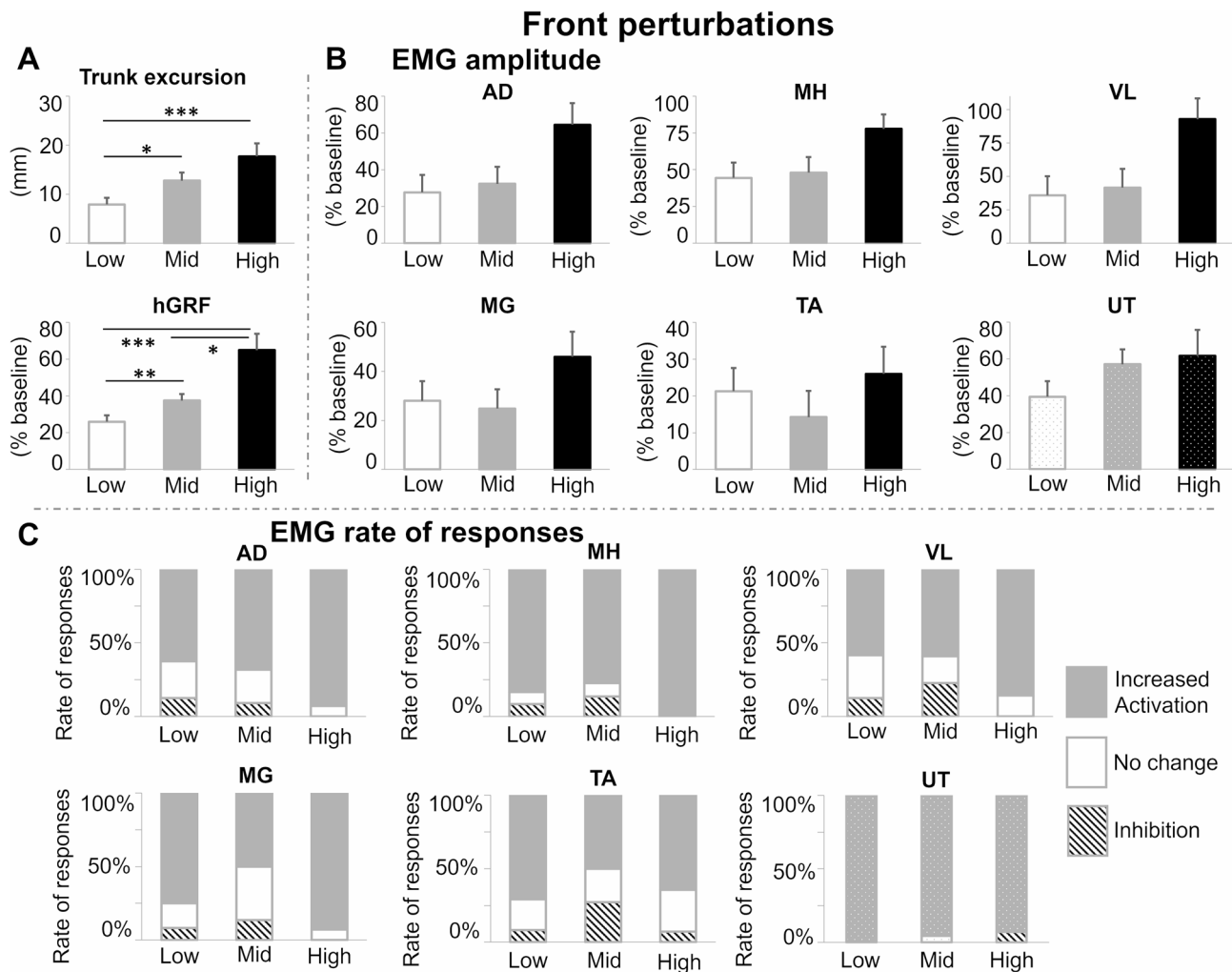


Fig. 6. Group averages during front trunk perturbations at Low, Mid and High magnitude for (A) trunk excursion and horizontal ground reaction force (hGRF), (B) electromyography (EMG) amplitude, and (C) rate of EMG response types. AD: adductor magnus; MH: medial hamstring; VL: vastus lateralis; MG: medial gastrocnemius; TA: anterior tibialis; UT: upper trapezius. Error bars represent the standard error. Successful attempts considered for analysis were 12 for Low, 11 for Mid, and 7 for High perturbations collected from 3 participants. Each attempt contributed to one data point for trunk excursion and two data points (i.e., left and right side) for ground reaction force and EMG amplitude. Significant difference: * $p < 0.05$; ** $p < 0.01$; *** $p < 0.001$.

even a decrease in EMG amplitude could occur at higher leg loading. Overall, the changes in lower limb EMG activity observed for the first time here during graded postural perturbations are consistent with the literature in that, after a motor complete SCI, the lumbosacral spinal cord can interpret load-related sensory information. However, characteristics of spinal cord sensory-motor processing that relate sensory input and motor output promoted by scES remain to be elucidated.

A significant and functionally relevant activation pattern was observed during back perturbations for antagonist ankle muscles (Figs. 4 and 5B). Higher perturbation magnitudes progressively decreased EMG amplitude of MG while trends of increased EMG amplitude were detected for TA. Such activation pattern modulation diverges from that often observed with augmented instability in able-bodied populations, in particular with aging and disuse, where increased levels of co-activation of antagonist muscles are implemented as a strategy to increase joint stiffness and improve overall postural stability^{42–44}. Further, during front perturbations, it is worth mentioning the statistical trend of increased EMG amplitude of VL and AD elicited by High magnitude (Fig. 6B). Sensory information related to horizontal GRF and hip stretch-sensitive afferents are two of the potential contributors for the described EMG amplitude modulations^{45,46}. Back and front trunk displacement results in stretching of the anterior and posterior muscle chain, respectively, which can project critical inputs for locomotion and postural control to the spinal cord after SCI^{20,46}. In particular, stretch receptors (muscle spindles) have been indicated as one of the primary afferent inputs to control postural reactions in animal models on a tilting platform²⁰. From a mechanistic perspective, the opposite relationship demonstrated by TA and MG between their EMG amplitude and the magnitude of back perturbations suggests that the available

ensembles of sensory information progressively engaged excitatory and inhibitory interneurons projecting to TA and MG motor pools, respectively, resulting in their opposite EMG amplitude trends (Figs. 4 and 5B). It is worth noting that the reciprocal inhibition mechanism appears to be complementary and competitive to the co-activation of antagonist muscles, which may be modulated at the spinal level by Ia-interneurons^{44,47}. However, one of the limits of the present study is the inability to define which specific groups of interneurons and/or neural networks were involved in these and other sensory-motor responses to trunk perturbations.

Considering the limited sample size of this proof of principle study, we opted not to assess the statistical interaction between perturbation magnitudes and directions, which warrants future investigation. Further, the significant differences and large to huge effect sizes detected here should be interpreted while considering that the post-hoc statistical power achieved for some of the comparisons was low. In particular, low statistical power was consistently found for front perturbations, reflecting the lower number of participants ($n=3$) that were able to successfully control all three perturbation magnitudes in this direction. Thus, the outcomes herein reported should not be generalized to a broader SCI population, and larger studies are needed to confirm the size and significance of the differences that were found. It should be also mentioned that we were unable to assess postural responses without spinal cord stimulation because the participants began to experience symptoms of orthostatic hypotension when scES intensity was reduced or turned off, and requested to sit. The future involvement of research participants with a lower level of injury and less-impacted cardiovascular function may allow to fill this gap.

In spite of the abovementioned limitations, the findings of this study can have important implications for the understanding and improvement of residual postural control potential after human SCI. First, the ensemble of sensory information related to leg loading, horizontal GRF as well as trunk displacement substantially accounted for the EMG amplitude modulation of representative ankle muscles (MG and TA) during back perturbations only. Conversely, additional sensory-motor features that were not assessed in this study appear to play a relevant role in the control of EMG amplitude modulation for the other lower limb muscles and perturbation directions, which should be investigated in future studies. Also, the lack of changes in lower limb activation sometimes observed when trunk displacement and GRF were progressively modulated by the different perturbation magnitudes raises the question of whether, and to what extent, increased joints stiffness resulting from the tonic muscle activation promoted by Stand-scES may contribute to standing postural control without an active spinal processing of the perturbative sensory information. The second aspect to consider is related to the criteria for the selection of perturbation magnitude within a potential activity-based training protocol for the recovery of postural control. Here, we showed that relatively small changes in trunk perturbation magnitude may or may not elicit relevant modulation in lower limb activation pattern while the postural control outcome was still successful. This is important because the characteristics of motor recovery achieved *via* training-induced neural plasticity depend on the sensory-motor patterns repeatedly practiced.

In conclusion, the proposed robotic framework allowed individuals with high-level motor complete SCI receiving Stand-scES to stand with free hands while delivering graded trunk perturbative forces that resulted in progressively larger trunk excursion and GRF modulation. The related spinal sensory-motor processing was less consistent. High-magnitude perturbations promoted certain leg EMG amplitude responses that were higher or lower than those deriving from Low- and Mid-perturbation magnitudes, depending on muscle and perturbation direction. In other instances, there was a lack of lower limb EMG amplitude modulation associated with progressively larger trunk displacement and GRF, which may question the contribution of an active sensory-motor processing for such combinations of muscles and perturbation directions. Thus, several aspects of the residual human spinal postural control potential remain to be elucidated. However, from an interventional point of view, we would suggest that the selection of perturbation magnitude for activity-based training should be based both on functional outcomes (i.e., safe, challenging and successfully controlled perturbations) and characteristics of lower limb activation patterns that should be strengthened.

Data availability

Data that supports the findings herein reported will be made available through material transfer agreement upon reasonable request.

Received: 1 September 2025; Accepted: 23 December 2025

Published online: 09 January 2026

References

1. Rejc, E., Angeli, C. & Harkema, S. Effects of lumbosacral spinal cord epidural stimulation for standing after chronic complete paraparesis in humans. *PloS One*. **10**, e0133998 (2015).
2. Harkema, S. et al. Effect of epidural stimulation of the lumbosacral spinal cord on voluntary movement, standing, and assisted stepping after motor complete paraplegia: a case study. *Lancet* **377**, 1938–1947 (2011).
3. Angeli, C. A. et al. Recovery of over-ground walking after chronic motor complete spinal cord injury. *N. Engl. J. Med.* (2018).
4. Gill, M. L. et al. Neuromodulation of lumbosacral spinal networks enables independent stepping after complete paraplegia. *Nat. Med.* (2018).
5. Rowald, A. et al. Activity-dependent spinal cord neuromodulation rapidly restores trunk and leg motor functions after complete paraparesis. *Nat. Med.* (2022).
6. Moraud, E. M. et al. Mechanisms underlying the neuromodulation of spinal circuits for correcting gait and balance deficits after spinal cord injury. *Neuron* **89**, 814–828 (2016).
7. Wenger, N. et al. Spatiotemporal neuromodulation therapies engaging muscle synergies improve motor control after spinal cord injury. *Nat. Med.* **22**, 138–145 (2016).
8. Capogrosso, M. et al. A computational model for epidural electrical stimulation of spinal sensorimotor circuits. *J. Neurosci.* **33**, 19326–19340 (2013).

9. Ladenbauer, J., Minassian, K., Hofstoetter, U. S., Dimitrijevic, M. R. & Rattay, F. Stimulation of the human lumbar spinal cord with implanted and surface electrodes: a computer simulation study. *IEEE Trans. Neural Syst. Rehabil Eng.* **18**, 637–645 (2010).
10. Edgerton, V. R., Tillakaratne, N. J., Bigbee, A. J., de Leon, R. D. & Roy, R. R. Plasticity of the spinal neural circuitry after injury. *Annu. Rev. Neurosci.* **27**, 145–167 (2004).
11. Rejc, E. & Angeli, C. A. Spinal cord epidural stimulation for lower limb motor function recovery in individuals with motor complete spinal cord injury. *Phys. Med. Rehabil. Clin. N Am.* **30**, 337–354 (2019).
12. Angeli, C. A., Edgerton, V. R., Gerasimenko, Y. P. & Harkema, S. J. Altering spinal cord excitability enables voluntary movements after chronic complete paralysis in humans. *Brain* **137**, 1394–1409 (2014).
13. Massion, J., Alexandrov, A. & Frolov, A. Why and how are posture and movement coordinated? *Prog Brain Res.* **143**, 13–27 (2004).
14. Lyalka, V. F., Orlovsky, G. N. & Deliagina, T. G. Impairment of postural control in rabbits with extensive spinal lesions. *J. Neurophysiol.* **101**, 1932–1940 (2009).
15. Beloozerova, I. N., Sirota, M. G., Orlovsky, G. N. & Deliagina, T. G. Activity of pyramidal tract neurons in the Cat during postural corrections. *J. Neurophysiol.* **93**, 1831–1844 (2005).
16. Beloozerova, I. N. et al. Postural control in the rabbit maintaining balance on the tilting platform. *J. Neurophysiol.* **90**, 3783–3793 (2003).
17. Deliagina, T. et al. Role of different sensory inputs for maintenance of body posture in sitting rat and rabbit. *Mot. Control.* **4**, 439–452 (2000).
18. Deliagina, T. G., Orlovsky, G. N., Zelenin, P. V. & Beloozerova, I. N. Neural bases of postural control. *Physiol. (Bethesda)* **21**, 216–225 (2006).
19. Musienko, P. E. et al. Regulation of posture and locomotion in decerebrate and spinal animals. *Neurosci. Behav. Physiol.* **45**, 229–237 (2015).
20. Musienko, P. E., Zelenin, P. V., Orlovsky, G. N. & Deliagina, T. G. Facilitation of postural limb reflexes with epidural stimulation in spinal rabbits. *J. Neurophysiol.* **103**, 1080–1092 (2010).
21. Musienko, P. et al. Somatosensory control of balance during locomotion in decerebrated Cat. *J. Neurophysiol.* **107**, 2072–2082 (2012).
22. Lyalka, V. F. et al. Facilitation of postural limb reflexes in spinal rabbits by serotonergic agonist administration, epidural electrical stimulation, and postural training. *J. Neurophysiol.* **106**, 1341–1354 (2011).
23. Rejc, E. et al. Robotic postural training with epidural stimulation for the recovery of upright postural control in individuals with motor complete spinal cord injury: a pilot study. *Neurotrauma Rep.* **5**, 277–292 (2024).
24. Khan, M. et al. Stand trainer with applied forces at the pelvis and trunk: response to perturbations and Assist-As-Needed support. *IEEE Trans. Neural Syst. Rehabil Eng.* **27**, 1855–1864 (2019).
25. Bowersock, C. D. et al. Standing reactive postural responses of lower limbs with and without self-balance assistance in individuals with spinal cord injury receiving epidural stimulation. *J. Neurotrauma* (2023).
26. Rejc, E. et al. Effects of robotic postural stand training with epidural stimulation on sitting postural control in individuals with spinal cord injury: a pilot study. *J. Clin. Med.* **2024**, 13 (2024).
27. Rejc, E., Angeli, C. A., Bryant, N. & Harkema, S. J. Effects of stand and step training with epidural stimulation on motor function for standing in chronic complete paraplegics. *J. Neurotrauma* **34**, 1787–1802 (2017).
28. Ibáñez, J., Angeli, C. A., Harkema, S. J., Farina, D. & Rejc, E. Recruitment order of motor neurons promoted by epidural stimulation in individuals with spinal cord injury. *J. Appl. Physiol.* **131**, 1100–1110 (2021).
29. Angeli, C. et al. Targeted selection of stimulation parameters for restoration of motor and autonomic function in individuals with spinal cord injury. *Neuromodul. Technol. Neural Interface* (2023).
30. Sayenko, D. G., Angeli, C., Harkema, S. J., Edgerton, V. R. & Gerasimenko, Y. P. Neuromodulation of evoked muscle potentials induced by epidural spinal-cord stimulation in paralyzed individuals. *J. Neurophysiol.* **111**, 1088–1099 (2014).
31. Mesbah, S., Angeli, C. A., Keynton, R. S., El-Baz, A. & Harkema, S. J. A novel approach for automatic visualization and activation detection of evoked potentials induced by epidural spinal cord stimulation in individuals with spinal cord injury. *PLoS One.* **12**, e0185582 (2017).
32. Rattay, F., Minassian, K. & Dimitrijevic, M. R. Epidural electrical stimulation of posterior structures of the human lumbosacral cord: 2. quantitative analysis by computer modeling. *Spinal Cord.* **38**, 473–489 (2000).
33. Jilge, B. et al. Initiating extension of the lower limbs in subjects with complete spinal cord injury by epidural lumbar cord stimulation. *Exp. Brain Res.* **154**, 308–326 (2004).
34. Bowersock, C. D. et al. Robotic upright stand trainer (RobUST) and postural control in individuals with spinal cord injury. *J. Spinal Cord Med.* **2022**, 1–11 (2022).
35. Carpenter, M. G., Allum, J. H. & Honegger, F. Directional sensitivity of stretch reflexes and balance corrections for normal subjects in the roll and pitch planes. *Exp. Brain Res.* **129**, 93–113 (1999).
36. Cohen, J. *Statistical Power Analysis for the Behavioral Sciences* (L. Erlbaum Associates, 1988).
37. Sawilowsky, S. S. New effect size rules of thumb. *J. Mod. Appl. Stat. Methods.* **8**, 597–599 (2009).
38. Edgerton, V. R. & Roy, R. R. Activity-dependent plasticity of spinal locomotion: implications for sensory processing. *Exerc. Sport Sci. Rev.* **37**, 171–178 (2009).
39. Roy, R., Harkema, S. & Edgerton, V. Basic concepts of activity-based interventions for improved recovery of motor function after spinal cord injury. *Arch. Phys. Med. Rehabil.* **93**, 1487–1497 (2012).
40. Rejc, E., Angeli, C. A., Atkinson, D. & Harkema, S. J. Motor recovery after activity-based training with spinal cord epidural stimulation in a chronic motor complete paraplegic. *Sci. Rep.* **7**, 13476 (2017).
41. Harkema, S. J. et al. Human lumbosacral spinal cord interprets loading during stepping. *J. Neurophysiol.* **77**, 797–811 (1997).
42. Hortobágyi, T. & DeVita, P. Muscle pre- and coactivity during downward stepping are associated with leg stiffness in aging. *J. Electromyogr. Kinesiol.* **10**, 117–126 (2000).
43. Onambélé, G. L., Narici, M. V., Rejc, E. & Maganaris, C. N. Contribution of calf muscle-tendon properties to single-leg stance ability in the absence of visual feedback in relation to ageing. *Gait Posture.* **26**, 343–348 (2007).
44. Latash, M. L. Muscle coactivation: definitions, mechanisms, and functions. *J. Neurophysiol.* **120**, 88–104 (2018).
45. Horak, F. B., Henry, S. M. & Shumway-Cook, A. Postural perturbations: new insights for treatment of balance disorders. *Phys. Ther.* **77**, 517–533 (1997).
46. Onushko, T., Hyngstrom, A. & Schmit, B. D. Hip proprioceptors preferentially modulate reflexes of the leg in human spinal cord injury. *J. Neurophysiol.* **110**, 297–306 (2013).
47. Nielsen, J. B. Human spinal motor control. *Annu. Rev. Neurosci.* **39**, 81–101 (2016).

Acknowledgements

We thank the research volunteers for their valuable contribution to this study. We also gratefully acknowledge our research staff for their contribution to data collection and our training staff for their support of the research volunteers; Dr Maxwell Boakye for surgical implantation and medical oversight; Dr Sarah Wagers for medical oversight; Yukishia Austin, Lynn Robbins, and Kristen Johnson for medical management; Be-U Analytics for professional statistical consultation and analytical support. This work was supported by Kessler Foundation,

Christopher and Dana Reeve Foundation, Leona M. & Harry B. Helmsley Charitable Trust, UofL Health - University of Louisville Hospital, and Medtronic Plc.

Author contributions

ER, SA, SJH, and CAA conceived research; ER and CDB designed research; ER, CDB, TP and CAA performed experiments; ER, CDB, TP and SZ analyzed data; ER, CDB and SZ prepared figures; ER, CDB, GFF, SJH and SA interpreted results of experiments; ER drafted the manuscript; and all authors edited, revised, and approved the final version of manuscript.

Funding

This study was funded by the New York State Spinal Cord Injury Research Board under the awards C31290GG and C37719GG.

Competing interests

The authors declare no competing interests.

Additional information

Supplementary Information The online version contains supplementary material available at <https://doi.org/10.1038/s41598-025-33907-6>.

Correspondence and requests for materials should be addressed to E.R.

Reprints and permissions information is available at www.nature.com/reprints.

Publisher's note Springer Nature remains neutral with regard to jurisdictional claims in published maps and institutional affiliations.

Open Access This article is licensed under a Creative Commons Attribution-NonCommercial-NoDerivatives 4.0 International License, which permits any non-commercial use, sharing, distribution and reproduction in any medium or format, as long as you give appropriate credit to the original author(s) and the source, provide a link to the Creative Commons licence, and indicate if you modified the licensed material. You do not have permission under this licence to share adapted material derived from this article or parts of it. The images or other third party material in this article are included in the article's Creative Commons licence, unless indicated otherwise in a credit line to the material. If material is not included in the article's Creative Commons licence and your intended use is not permitted by statutory regulation or exceeds the permitted use, you will need to obtain permission directly from the copyright holder. To view a copy of this licence, visit <http://creativecommons.org/licenses/by-nc-nd/4.0/>.

© The Author(s) 2026